CrystEngComm

Accepted Manuscript

This article can be cited before page numbers have been issued, to do this please use: C. J. Doonan, C. J. Sumby, T. Keene and D. Rankine, *CrystEngComm*, 2013, DOI: 10.1039/C3CE41253A.

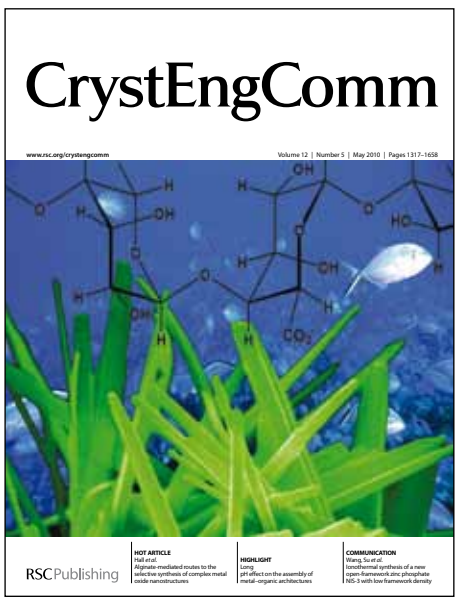

This is an *Accepted Manuscript*, which has been through the RSC Publishing peer review process and has been accepted for publication.

Accepted Manuscripts are published online shortly after acceptance, which is prior to technical editing, formatting and proof reading. This free service from RSC Publishing allows authors to make their results available to the community, in citable form, before publication of the edited article. This *Accepted Manuscript* will be replaced by the edited and formatted *Advance Article* as soon as this is available.

To cite this manuscript please use its permanent Digital Object Identifier (DOI®), which is identical for all formats of publication.

More information about *Accepted Manuscripts* can be found in the **Information for Authors**.

Please note that technical editing may introduce minor changes to the text and/or graphics contained in the manuscript submitted by the author(s) which may alter content, and that the standard **Terms & Conditions** and the **ethical guidelines** that apply to the journal are still applicable. In no event shall the RSC be held responsible for any errors or omissions in these *Accepted Manuscript* manuscripts or any consequences arising from the use of any information contained in them.

View Article Online
DOI: 10.1039/C3CE41253A

Chelation-driven fluorescence deactivation in three alkali earth metal MOFs containing 2,2'-dihydroxybiphenyl-4,4'-dicarboxylate

Damien Rankine,[a] Tony D. Keene,[ab] Christopher J. Sumby,[a*] and Christian J. Doonan[a*]

Received (in XXX, XXX) XthXXXXXXXXX 20XX, Accepted Xth XXXXXXXXX 20XX
DOI: 10.1039/b000000x

Three new metal-organic frameworks (MOFs) have been synthesised from alkali earth metal ions of increasing ionic radii (Mg, Ca and Sr) and 2,2'-dihydroxybiphenyl-4,4'-dicarboxylic acid (H_4diol). The distinct coordination environments, framework topologies and the non-coordinated diol moieties accessed are a result of using differently sized metal ions for MOF synthesis which affects the ability of the diol moieties to chelate the metal. Detailed structural analysis of $[Sr_3(H_2diol)_3(DMF)_5]$, $[Ca_{3.5}(Hdiol)(H_2diol)_2(DMF)_5]$.1.2DMF and $[Mg(H_2diol)(DMF)_2]$.DMF show distinctive variations in variable temperature expansion/contraction properties and porosity. In addition, $[Sr_3(H_2diol)_3(DMF)_5]$ and $[Ca_{3.5}(Hdiol)(H_2diol)_2(DMF)_5]$.1.2DMF display a broad fluorescence emission (λ_{max} = ~435 nm) under ultraviolet light due to the presence of non-coordinated biphenyl-diol moieties within the structures, while chelation of Mg by the diol pocket in $[Mg(H_2diol)(DMF)_2]$.DMF leads to quenching of the ligand fluorescence.

Introduction

Metal-organic frameworks (MOFs) are a rapidly growing class of materials that are known for their exceptionally high surface areas, diverse topologies and periodic structures.[1, 2] The first examples of permanently porous MOFs were composed of rigid phenylene moieties and metal carboxylate clusters that formed the links and nodes, respectively, of extended networks.[3-8] This modular synthetic approach facilitated the generation of a wide range of materials of predetermined topologies and structure metrics.[9] Subsequent to these seminal studies permanently porous frameworks constructed from more complex organic links that are inherently flexible, and/or possess multiple functionality, have been reported. MOFs synthesized from such links have led to the generation of open architectures with fundamentally interesting structural features such as, crystal-to-crystal 'breathing',[10, 11] gated adsorption[12-14] and coordinatively unsaturated metals sites.[14-17] Examples of the latter have demonstrated exceptional gas separation properties by virtue of their novel metal co-ordination environments. For example $[Mg_2(dobdc)]$ efficiently separates CO_2/CH_4 gas mixtures and the analogous Fe based MOF, $[Fe_2(dobdc)]$, exhibited excellent selectivity for alkane/alkene separations.[18-20]

Recently, we reported the synthesis of a Ni(II) based MOF, $[Ni(H_2diol)(DMF)_2]$, constructed from the multidentate ligand 2,2'-dihydroxybiphenyl-4,4'-dicarboxylic acid (H_4diol).[21, 22] The rotational mobility about the phenyl moieties combined with the rigid backbone gave rise to a chiral quartz topology that displayed novel solvent-modified dynamic porosity through rotation of axial DMF molecules on the octahedral Ni nodes. Upon removal of DMF the octahedral Ni site was converted to a coordinatively unsaturated 4-coordinate species that reversibly bound H_2O and MeOH. Building upon this work, we anticipated that topologically analogous frameworks could be synthesised from other divalent metals, and thus we sought to investigate the reaction of H_4diol with a series of alkali earth metals. Examples of group 2 alkali earth metals as connecting nodes in MOFs are relatively uncommon[23, 24] compared to first and second row transition metals.[25, 26] Our interest in the group 2 metals was motivated by examples of Mg-based MOFs exhibiting exceptional gas adsorption properties[2, 20] due to their low molecular weight and high charge density plus the relative abundance and low cost of these metals. Another driving factor for utilising group II metals is the lack of unpaired electrons, which would otherwise quench any potential fluorescence from the organic links. Fluorescent MOFs display possible applications in sensing where absorbed species can either chemi- or physisorb into the MOF and deactivate fluorescence as a highly sensitive means of detection.[27]

Herein, we report the synthesis of three new 3D MOFs, $[Sr_3(H_2diol)_3(DMF)_5]$, $[Ca_{3.5}(Hdiol)(H_2diol)_2(DMF)_5]$1.2DMF and $[Mg(H_2diol)(DMF)_2]$.DMF formed via from the combination of MCl_2 (where M = Sr, Ca or Mg) and 2,2'-dihydroxy-1,1'-biphenyl-4,4'-dicarboxylic acid (H_4diol)[21] under solvothermal conditions.[22] The $[Sr_3(H_2diol)_3(DMF)_5]$ and $[Ca_{3.5}(Hdiol)(H_2diol)_2(DMF)_5]$.1.2DMF structures possess uncoordinated diol moieties whereas $[Mg(H_2diol)(DMF)_2]$.DMF was found to be isostructural to $[Ni(H_2diol)(DMF)_2]$. These data suggest that the larger Ca and Sr metal ions prevent the octahedral coordination environment observed for Mg (and Ni), thus affording structures with free diol moieties and allowing solid-state MOF fluorescence. We describe the structures and explore the physical properties of this new series of alkali metal based MOFs.

Selected Experimental Details

Synthesis of Metal-Organic Frameworks

$[Sr_3(H_2diol)_3(DMF)_5]$and $[Ca_{3.5}(Hdiol)(H_2diol)_2(DMF)_5]$.1.2DMF were synthesised by the following solvothermal methods: $SrCl_2$ or $CaCl_2$ (0.1 mmol), H_4diol (0.1 mmol) and DABCO (0.055 mmol) were dissolved in DMF (1.0 mL) in a sealed glass tube and heated at 150°C for 16 hours yielding colourless, block crystals.$[Sr_3(H_2diol)_3(DMF)_5]$: Yield: 80%, FT-IR (cm^{-1}): 3495 (br.), 2938 (w), 1661 (s), 1538 (m), 1387 (s), 1256 (s), 1097 (s). Analysis calc. for $[Sr_3(H_2diol)_3(DMF)_5].0.5DMF.2H_2O$: C 46.83, H 5.36, N 7.59; Found C 46.26, H 5.17, N 8.01%.$[Ca_{3.5}(Hdiol)(H_2diol)_2(DMF)_5]$.1.2DMF: Yield: 76%, FT-IR (cm^{-1}): 3316 (br.), 2937 (w), 1661 (s), 1523 (m), 1396 (s), 1235 (s), 1104 (s). Analysis calc. for $[Ca_{3.5}(Hdiol)(H_2diol)_2(DMF)_5].5H_2O$: C 49.40, H 4.68, N 5.03; Found C 49.20, H 4.94, N 5.03%.

View Article Online
DOI: 10.1039/C3CE41253A

Table 1. Summary of the crystallographic data.

Compound	$[Sr_3(H_2diol)_3(DMF)_5]$	$[Ca_{3.5}(H_2diol)(H_2diol)_2(DMF)_5].1.2DMF$	$[Mg(H_2diol)(DMF)_2].DMF$
Formula	$C_{57}H_{59}Sr_3N_5O_{23}$	$C_{60.6}H_{66.4}Ca_{3.5}N_{6.2}O_{24.2}$	$C_{23}H_{29}MgN_3O_9$
Crystal system	Orthorhombic	Monoclinic	Trigonal
Space group	*Pbcn*	*C2/c*	$P3_221$
a/Å	27.3062(14)	43.986(2)	17.4446(8)
b/Å	19.4347(9)	14.1893(5)	17.4446(8)
c/Å	31.1766(2)	26.3617(17)	8.5897(5)
α/°	90	90	90
β/°	90	107.283(5)	90
γ/°	90	90	120
V/Å^3	16545.0(16)	15710.2(14)	2263.8(2)
ρ/g cm^{-3}	1.221	1.192	1.135
Z	8	8	3
T/K	150(2)	110(2)	150(2)
μ/mm^{-1}	1.994	0.314	0.106
Reflections collected	95073	87876	13027
Unique reflections (R_{int})	17986 (0.1008)	17095 (0.0517)	2968 (0.0557)
Reflections $I>2\sigma(I)$	10973	12199	2390
Data/Restraints/Parameters	17986 / 27 / 951	17095 / 75 / 820	2968 / 1 / 145
Goodness of fit (S)	1.043	1.267	1.102
R_1/wR_2 [$I>2\sigma(I)$]	0.0673 / 0.1631	0.0998 / 0.3052	0.0531 / 0.1436
R_1/wR_2 (all data)	0.1190 / 0.1813	0.1231 / 0.3275	0.0670 / 0.1532

$[Mg(H_2diol)(DMF)_2].DMF$: $MgCl_2$ (0.1 mmol), H_4diol (0.1 mmol) and DABCO (0.055 mmol) were dissolved in DMF (1.0 mL) in a capped glass scintillation vial and heated at 120°C for 8 hours yielding colourless, block crystals in ~ 50 % yield. FT-IR (cm^{-1}): 3344 (br.), 1659 (s), 1539 (m), 1386 (s), 1217 (s), 1106 (s). Analysis calc. for $[Mg(H_2diol)(DMF)_2].0.5DMF.4H_2O$: C 46.83, H 6.14, N 6.35; Found C 47.19, H 5.35, N 6.23%.

X-Ray Crystallography

Crystals were mounted under paratone-N oil on a plastic loop. X-ray diffraction data were collected with Mo-Kα radiation (λ = 0.7107 Å) using Oxford Diffraction X-calibur single crystal X-ray diffractometer at 150(2) or 110(2) K. Data sets were corrected for absorption using a multi-scan method, and structures were solved by direct methods using SHELXS-97[28] and refined by full-matrix least squares on F^2 by SHELXL-86,[29] interfaced through the program X-Seed.[30] In general, all non-hydrogen atoms were refined anisotropically and hydrogen atoms were included as invariants at geometrically estimated positions, unless specified otherwise in additional details below. Details of data collections and structure refinements are given below. CCDC numbers 915129, 945502 and 945503 contain the supplementary crystallographic data for this structure. These data can be obtained free of charge from The Cambridge Crystallographic Data Centre via www.ccdc.cam.ac.uk/data_request/cif.

Powder X-ray Diffraction

In-house powder X-ray diffraction data was collected on a Rigaku Hiflux Homelab system using Cu-Kα radiation with an R-Axis IV++ image plate detector. Samples were mounted on plastic loops using paratone-N and data collected by scanning 90° in phi for 120 second exposures. The data was converted into *xye* format using the program DataSqueeze. Simulated powder X-ray diffraction patterns were generated from the single crystal data using Mercury 2.4.

Results and Discussion

The structures of $[Sr_3(H_2diol)_3(DMF)_5]$ and $[Ca_{3.5}(Hdiol)(H_2diol)_2(DMF)_5].1.2DMF$ are composed of 1D oxygen-bridged metal chains connected by H_2diol ligands to form 3D, non-interpenetrated networks. In contrast, $[Mg(H_2diol)(DMF)_2]$ is best described as a 3D quartz-like lattice which is structurally analogous to the previously reported $[Ni(H_2diol)(DMF)_2]$.[22] All materials were synthesised by solvothermal methods in moderate to good yields from their corresponding metal(II) chloride salts and H_4diol. The structures of the resulting MOFs were characterised initially by single crystal X-ray crystallography and subsequently by powder X-ray diffraction (PXRD), elemental analysis and IR spectroscopy.

$[Sr_3(H_2diol)_3(DMF)_5]$ crystallises as colourless blocks in the orthorhombic space group *Pbcn* with the formula $C_{57}H_{61}O_{21}N_5Sr_3$. The asymmetric unit consists of three 8-coordinate Sr(II) atoms of distorted dodecahedral geometry, the equivalent of three H_2diol ligands with either mono- or bidentate coordination by each carboxylate group, and a total of five coordinated DMF molecules, one of which adopts a μ_2-bridging coordination mode. Two distinct modes of carboxylate coordination are evident in $[Sr_3(H_2diol)_3(DMF)_5]$: (i) chelation to a single Sr(II) ion, whereby each carboxylate oxygen has a μ_2-coordination mode and also bridges to an adjacent Sr(II) ion or, (ii) simple monodentate coordination of a Sr centre by a single carboxylate oxygen from the carboxylate group (Fig 1). In this latter case the remaining carboxylate oxygen is non-coordinating but within hydrogen-bonding distance to an adjacent H_2diol OH group, with an O–O distance of 2.570 Å. The combination of these coordination and hydrogen-bonding effects provides a robust connectivity. Twisting of H_2diol about the biaryl axis occurs for all ligands in the structure, with biaryl dihedral angles of 50.5(8), 54.9(8) and 63.4(9)°. This twisting allows the carboxylates to maintain resonance stability with the aryl ring whilst retaining an optimal chelating position in the structure. An average carboxylate C–O distance of 1.254(6) Å indicates charge delocalisation across the carboxylate and confirms deprotonation. Greater variation in bond lengths for the Sr(II) MOF occurs with Sr–O bond lengths ranging from 2.453(7) to 2.767(3) Å, compared with Ca–O bonds which range from 2.313(4) to

View Article Online
DOI: 10.1039/C3CE41253A

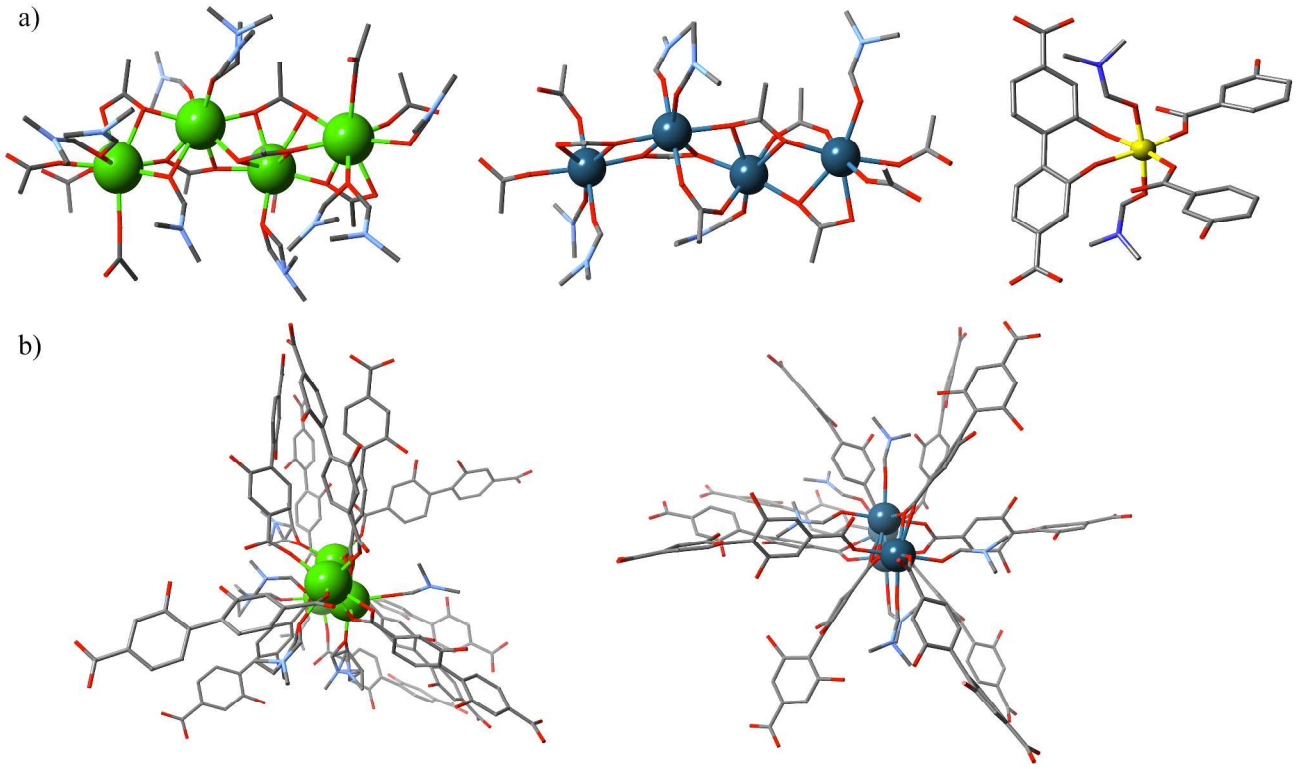

Figure 1. a) Local coordination environment for (left to right) $[Sr_3(H_2diol)_3(DMF)_5]$, $[Ca_{3.5}(Hdiol)(H_2diol)_2(DMF)_5].1.2DMF$ and $[Mg(H_2diol)(DMF)_2].DMF$, and b) views down the metal-oxide chain for $[Sr_3(H_2diol)_3(DMF)_5]$ and $[Ca_{3.5}(Hdiol)(H_2diol)_2(DMF)_5].1.2DMF$. Atom colours: Sr – green, Ca – dark blue, Mg – yellow, C – grey, N – light blue, O- red. Hydrogen atoms have been removed for clarity.

2.540(3) Å in $[Ca_{3.5}(Hdiol)(H_2diol)_2(DMF)_5].1.2DMF$. The larger range of bond lengths is a likely consequence of the non-symmetrical coordination environment surrounding each Sr(II) atom, as well as the variations in coordinating species and ionic radii of the metal ion.

The $[Sr_3(H_2diol)_3(DMF)_5]$ network consists of linear polymeric Sr–O chains which are bridged by H_2diol ligands to form a 3D framework (Fig. 1). Notably, this structure possesses non-coordinated diol groups pointing into the pore cavities. Small, highly constricted pore channels can be seen when the structure is examined down the b-axis, aligned with the linear Sr–O chains. From all other axes, coordinated DMF molecules restrict access to the pores.

$[Ca_{3.5}(Hdiol)(H_2diol)_2(DMF)_5].1.2DMF$ crystallises as colourless plates in the monoclinic space group *C*2/*c* with the formula $C_{57}H_{58}O_{23}N_5Ca_{3.5}$. The asymmetric unit consists of one 6-coordinate Ca(II) centre, with two longer Ca–O contacts at ~2.73Å, and three 7-coordinate Ca(II) ions that adopt a pentagonal bipyramidal geometry (Fig. 1). In addition, two H_2diol and one Hdiol ligands are present along with five coordinated DMF molecules. Careful analysis of the structure using PLATON indicated an additional 382e^- in the unit cell, corresponding to 1.2 DMF molecules per formula unit. The biaryl dihedral angles observed in the structure of $[Ca_{3.5}(Hdiol)(H_2diol)_2(DMF)_5].1.2DMF$ of 43.1(8), 43.2(8) and 61(1)° are close to the equivalent angles in $[Sr_3(H_2diol)_3(DMF)_5]$. Analogous to the Sr MOF, the carboxylate groups in $[Ca_{3.5}(Hdiol)(H_2diol)_2(DMF)_5].1.2DMF$ are co-planar with the phenyl rings in order to maintain delocalisation. Furthermore, the carboxylate C–O and C=O distances range from 1.243(5) to 1.265(4) Å, respectively, which closely match those in $[Sr_3(H_2diol)_3(DMF)_5]$. In contrast to $[Sr_3(H_2diol)_3(DMF)_5]$, the H_2diol carboxylates are fully coordinated in $[Ca_{3.5}(Hdiol)(H_2diol)_2(DMF)_5].1.2DMF$ and each oxygen acts as a μ_2 bridging donor, the longer of these bonds occurs within the four membered chelate rings formed when the carboxylate group binds to a Ca(II) ion, while the shorter is observed when a carboxylate oxygen bridges to a second Ca(II) centre.

The framework connectivity of $[Ca_{3.5}(Hdiol)(H_2diol)_2(DMF)_5].1.2DMF$ possesses similar features to $[Sr_3(H_2diol)_3(DMF)_5]$. For example, $[Ca_{3.5}(Hdiol)(H_2diol)_2(DMF)_5].1.2DMF$ contains 1D Ca–O chains that run down the *c*-axis of the material and these are bridged by H_2diol ligands (Fig. 1). However, in contrast to $[Sr_3(H_2diol)_3(DMF)_5]$, $[Ca_{3.5}(Hdiol)(H_2diol)_2(DMF)_5].1.2DMF$ is non-porous and any potential voids within the structure are filled with coordinated DMF molecules. Close inspection of the structures of both $[Sr_3(H_2diol)_3(DMF)_5]$ and $[Ca_{3.5}(Hdiol)(H_2diol)_2(DMF)_5].1.2DMF$, show that the free diol groups are oriented in the same direction, showing a preference for inter-ligand hydrogen bonding, rather than interaction with pore solvents.

$[Mg(H_2diol)(DMF)_2].DMF$ crystallises as a racemic mixture of colourless crystals in the enantiomorphic space group pair - $P3_121$ and $P3_221$. This structure is analogous to the quartz-like topology determined for $[Ni(H_2diol)(DMF)_2]$.[22] $[Mg(H_2diol)(DMF)_2].DMF$ exhibits a double-helical pore structure along the c-axis, defining the basis of chirality in the structure as axial chirality in the biaryl bond. The asymmetric unit contains one octahedral Mg(II) centre, half of one H_2diol ligand and one coordinated DMF molecule. Two equivalents of the doubly deprotonated H_2diol ligand are coordinated to the

View Article Online
DOI: 10.1039/C3CE41253A

octahedral Mg(II) ions through a single carboxylate oxygen donor and a third H_2diol ligand chelates through the diol moiety. The ligand coordination environment about the Mg(II) centre constitutes a local *xy* plane with two coordinated DMF molecules in the axial sites of the O_h metal centre. Structural analysis by PLATON indicated an additional 131e$^-$, corresponding to one DMF molecule per formula unit. The Mg(II) centre is further stabilised by hydrogen bonding interactions between non-coordinating oxygen atoms of the carboxylate group. It is noteworthy that this hydrogen bond was located by single-crystal X-ray crystallography in a well-defined position between the two non-coordinating oxygen atoms.

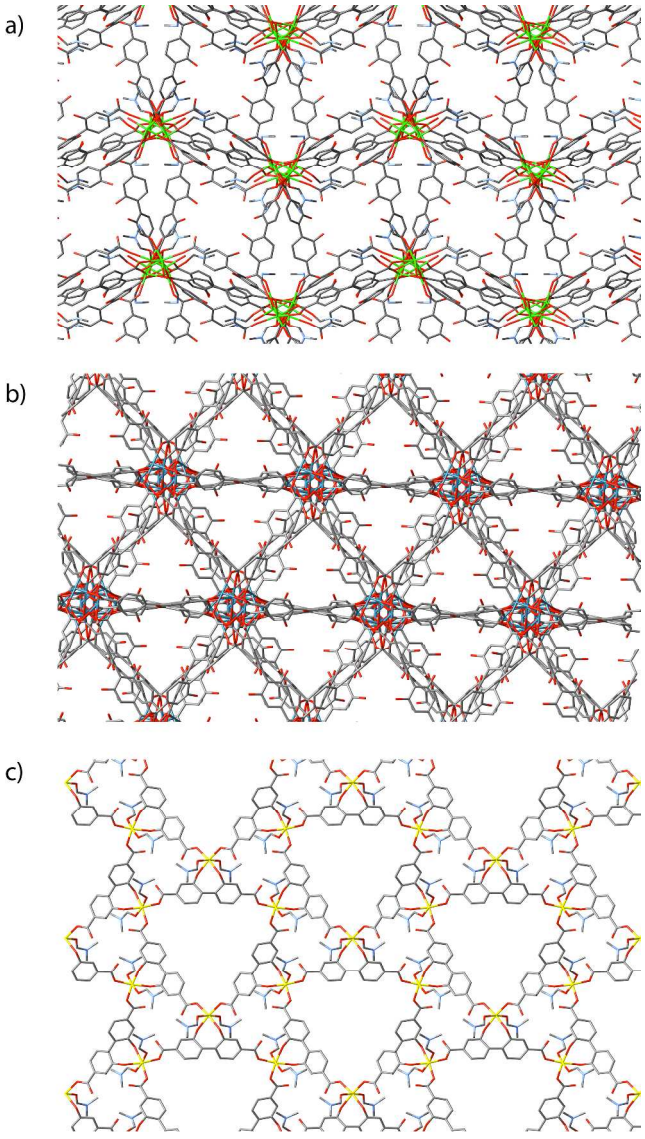

Figure 2. Images displaying the pore environment and extended structures of a) $[Sr_3(H_2diol)_3(DMF)_5]$ (*c*-axis), b) $[Ca_{3.5}(Hdiol)(H_2diol)_2(DMF)_5]$.1.2DMF (101 axis, coordinated DMF molecules removed for clarity) and c) $[Mg(H_2diol)(DMF)_2]$.DMF (*c*-axis). Atom colours: Sr – green, Ca – dark blue, Mg – yellow, C – grey, N – light blue, O- red. Hydrogen atoms have been removed for clarity.

The MOF structures formed with these group II metal ions show a preference for higher coordination numbers descending down the group from Mg(II) to Sr(II). The natural bite angle observed in $[Mg(H_2diol)(DMF)_2]$.DMF is approximately 90°, as expected for a typical O_h complex, with an O−O distance of 2.8 Å.

Despite the rotational flexibility of the biaryl link, chelation was only observed in the structure of $[Mg(H_2diol)(DMF)_2]$.DMF and not in those of $[Sr_3(H_2diol)_3(DMF)_5]$ and $[Ca_{3.5}(Hdiol)(H_2diol)_2(DMF)_5]$.1.2DMF. The lack of diol chelation to the metal cations of larger ionic radii may be due to several factors including; coordinating molecules in solution (i.e. DMF), synthesis temperature and reagent concentration, and, most likely, the energy barrier involved with forming the chelate ring. The ionic radii increases down group 2, from 0.720 Å for Mg(II) to 1.26 Å for Sr(II) along with the M–O bond lengths. Thus diol chelation of the larger cations would result in an unfavourable bite angle and ligand geometry. Selective diol chelation in these MOFs can thus be achieved by judicious choice of metal ion size and this may prove to be an effective strategy for selectively accessing free diol groups in MOFs formed from particular metals withoutthe need for protecting groups.

Whilst all three MOFs could be synthesised under identical conditions at 120°C, it was shown that both $[Sr_3(H_2diol)_3(DMF)_5]$ and $[Ca_{3.5}(Hdiol)(H_2diol)_2(DMF)_5]$.1.2DMF could be synthesised with higher yields at 150°C, whereas $[Mg(H_2diol)(DMF)_2]$.DMF showed improved crystal growth and yield at 100°C. Powder X-ray diffraction (PXRD) methods were used to confirm phase purity of $[Sr_3(H_2diol)_3(DMF)_5]$, $[Ca_{3.5}(Hdiol)(H_2diol)_2(DMF)_5]$.1.2DMF and $[Mg(H_2diol)(DMF)_2]$ (Fig. 3). Le Bail refinement of the experimental PXRD data (ESI Fig. S3 - 5) confirmed that these correspond well to the calculated patterns generated from their respective single crystal structures. We note that activated $[Mg(H_2diol)(DMF)_2]$ was shown to maintain crystallinity upon removal of pore solvents, as well as upon solvent exchange with MeOH and subsequent desolvation at 200°C (Fig. 3). However, a loss of crystallinity is observed upon removal of pore solvent for $[Sr_3(H_2diol)_3(DMF)_5]$ and $[Ca_{3.5}(Hdiol)(H_2diol)_2(DMF)_5]$.1.2DMF. It is possible that the bridging mode of the DMF seen in $[Sr_3(H_2diol)_3(DMF)_5]$ renders this MOF particularly vulnerable to collapse on complete desolvation. Interestingly, this represents the first reported occurrence of a bridging DMF with Sr, while a small handful of DMF-bridged Ca species are reported in the CSD (CSD version 5.34 – Nov 2012).

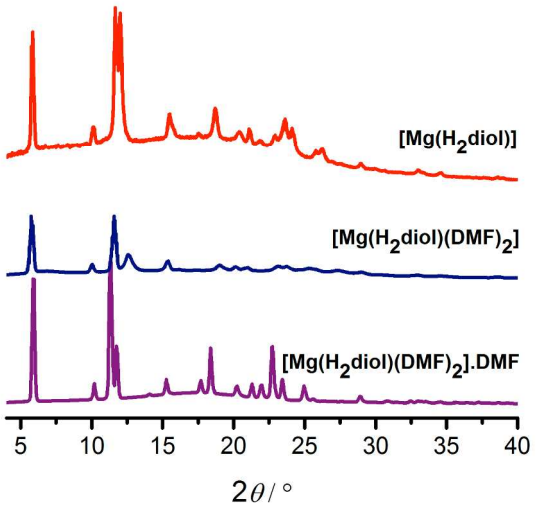

Figure 3. Powder X-ray diffraction patterns for the Mg (II) MOF.

Prediction of accessible surface areas was undertaken in order to estimate the potential porosity of each material. Predicted BET

View Article Online
DOI: 10.1039/C3CE41253A

surface areas of 126 and 144 m^2g^{-1} and maximum pore apertures of 1.8 and 4.0 Å, were calculated for $[Ca_{3.5}(Hdiol)(H_2diol)_2(DMF)_5]$ and $[Sr_3(H_2diol)_3(DMF)_5]$, respectively. The predicted BET surface area for $[Mg(H_2diol)(DMF)_2]$ was calculated to be 1064 m^2g^{-1}. The higher predicted surface area of the Mg(II) analogue, over $[Sr_3(H_2diol)_3(DMF)_5]$ and $[Ca_{3.5}(Hdiol)(H_2diol)_2(DMF)_5]$ can be attributed to the large hexagonal channels oriented along the crystallographic *c*-axis. A 77 K N_2 isotherm was carried out on bulk samples of $[Mg(H_2diol)(DMF)_2]$ yielding an experimental BET surface area of 390 m^2g^{-1} (ESI Fig. S1). In our hands, $[Sr_3(H_2diol)_3(DMF)_5]$ and $[Ca_{3.5}(Hdiol)(H_2diol)_2(DMF)_5]$ were found to be non-porous under the activation conditions employed. For $[Mg(H_2diol)(DMF)_2]$ this smaller than expected surface area may be attributed to some crystal degradation upon activation, which is supported by a loss in crystallinity.

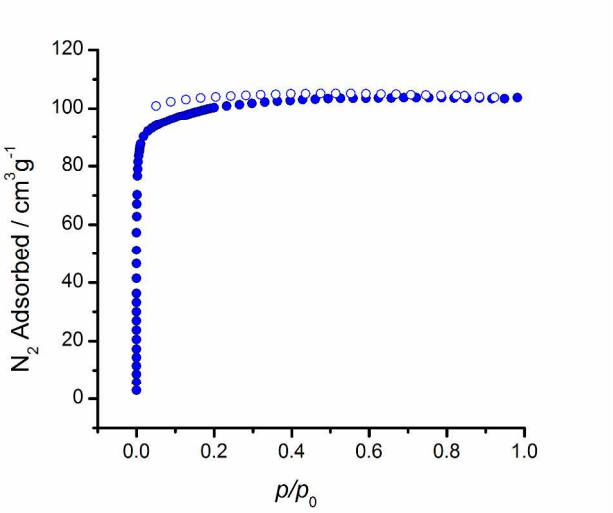

Figure 4. N_2 adsorption isotherm at 77K for $[Mg(H_2diol)(DMF)_2]$.

Thermogravimmetric analysis (TGA) was utilised to assess the thermal properties of each MOF (ESI, Fig. S5 - 7). The TGA trace of $[Mg(H_2diol)(DMF)_2].DMF$ showed sharp loss of pore DMF up to 200°C, followed by a plateau and the onset of structural decomposition at ~390°C.For $[Sr_3(H_2diol)_3(DMF)_5]$ and $[Ca_{3.5}(Hdiol)(H_2diol)_2(DMF)_5].1.2DMF$ the loss of pore guest molecules was observed from 120 – 200°C. This was followed by a slow decrease in mass to 400°C, and finally the onset of structural decomposition from 450°C. Due to the relatively featureless nature of the TGA trace for $[Sr_3(H_2diol)_3(DMF)_5]$ and $[Ca_{3.5}(Hdiol)(H_2diol)_2(DMF)_5].1.2DMF$ it is difficult to draw accurate conclusions regarding thermal stability. In order to further assess the temperature-dependent crystallinity and thermal stability of each MOF, we performed variable-temperature X-ray diffraction (VT-XRD) experiments. These data indicated that both $[Ca_{3.5}(Hdiol)(H_2diol)_2(DMF)_5].1.2DMF$ and $[Sr_3(H_2diol)_3(DMF)_5]$ structures lose single crystallinity at approximately 390 K and 430 K, respectively (ESI, Fig. S8 - 10). Continued loss of crystal transparency and diffraction intensity was observed above these temperatures. Over the temperature range 150 – 450 K, $[Ca_{3.5}(Hdiol)(H_2diol)_2(DMF)_5].1.2DMF$ and $[Sr_3(H_2diol)_3(DMF)_5]$ both display zero thermal expansion, along all axes, whereas $[Mg(H_2diol)(DMF)_2].DMF$ shows marked positive thermal expansion along the *c*-axis (Fig. 5).

Previously we have used transition metal-doping experiments to infer the presence of free diols within a MOF structure.[21] According to these methods, as-synthesised $[Sr_3(H_2diol)_3(DMF)_5]$was soaked in solutions of $CoCl_2$ or $CuCl_2$ (MeOH, DMF or acetone solutions) at various temperatures (25, 50 and 65°C) and concentrations (0.1, 1.0 and 5.0M). These experiments did not afford a persistent colour change in the transparent, colourless crystals of $[Sr_3(H_2diol)_3(DMF)_5]$ – thus confirming that the diol groups are inaccessible to post-synthetic modification under these conditions. We concluded that this is due to the small pore size compared to that of a $[(M)(solvent)_6]^{2+}$ ion preventing percolation of the metal salt through the crystal.

Biaryl compounds containing a 2,2'-dihydroxy motif, such as BINOL, are known to show interesting environment-modulated fluorescence emission properties.[33, 34] It is therefore expected that H_2diol would display this property when coordinated within an extended coordination network.

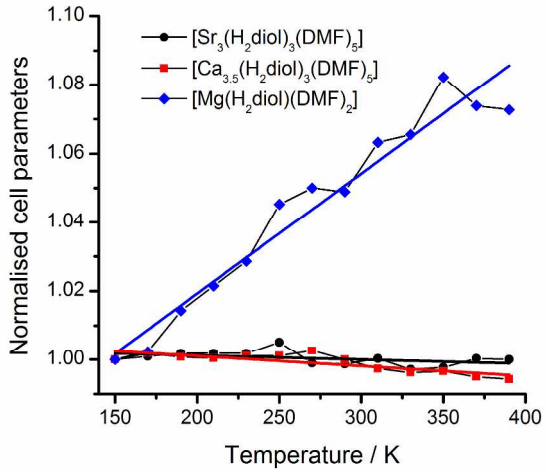

Figure 5. Changes in cell parameters along the c-axis for $[Sr_3(H_2diol)_3(DMF)_5]$ (black), $[Ca_{3.5}(Hdiol)(H_2diol)_2(DMF)_5].1.2DMF$ (red) and $[Mg(H_2diol)(DMF)_2].DMF$ (blue) from variable-temperature X-ray diffraction data.

Solid-state fluorescence spectroscopy was performed on all three MOFs, as well as the free H_4diol ligand, at an excitation wavelength of 240 nm (Fig. 6). A distinctive fluorescent response was observed for MOFs with exposed diol groups, $[Sr_3(H_2diol)_3(DMF)_5]$ and $[Ca_{3.5}(Hdiol)(H_2diol)_2(DMF)_5].1.2DMF$, yet was not observed for $[Mg(H_2diol)(DMF)_2].DMF$. Fluorescence spectra of $[Sr_3(H_2diol)_3(DMF)_5]$and $[Ca_{3.5}(Hdiol)(H_2diol)_2(DMF)_5].1.2DMF$ both show a broad ligand-based emission peak at λ = 435 nm. Quenching of fluorescence emission was observed for $[Mg(H_2diol)(DMF)_2].DMF$ due to chelation of the diol moiety in the MOF structure. In addition, quenching was also observed in the free H_4diol ligand due to its particular solid-state molecular packing. The free diol ligand does, however, display strong fluorescence when dissolved in polar aprotic solvents, such as DMF or DMSO, as well as in a 1:2:0.5 mixture of 10 M NaOH/THF/MeOH (ESI, Figure S12).

View Article Online
DOI: 10.1039/C3CE41253A

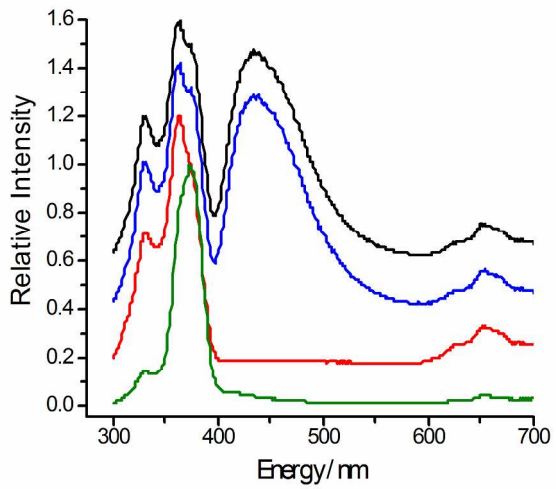

Figure 6. Solid-state fluorescence emission spectra for $[Sr_3(H_2diol)_3(DMF)_5]$ (black), $[Ca_{3.5}(Hdiol)(H_2diol)_2(DMF)_5].1.2DMF$ (blue), $[Mg(H_2diol)(DMF)_2].DMF$ (red) and H_4diol ligand (green). Spectra stacked for clarity.

Conclusions

Structural analysis of three alkali-earth metal based MOFs shows that the framework topology is dependent on the radii of the metal ions. Structures obtained from the smallest metal ion, Mg(II), have chelation of the metal ion by the H_2diol ligand, whereas the larger Ca(II) and Sr(II) ions do not chelate the diol groups. Interestingly, these frameworks with free diol groups lining the pores display solid-state fluorescence. While the highly restricted pore size of the Ca(II) and Sr(II) MOFs prevented the post-synthetic modification of the diol pockets, these compounds nonetheless highlight a route to fluorescent MOFs that may have applications in gas adsorbate sensing.

Notes and references

[a] *School of Chemistry and Physics, The University of Adelaide, SA 5005, Australia. CJD: Phone+61 8 8313 5770. Fax. +61 8 8313 4358.Email: christian.doonan@adelaide.edu.au; CJS: Phone +61 8 8313 7406. Fax. +61 8 8313 4358.Email: christopher.sumby@adelaide.edu.au*
[b] *Present address: School of Chemistry, University of Southampton, University Road, Southampton, SO17 1BJ, UK.*
* *Corresponding Author*

† Electronic Supplementary Information (ESI) available: additional experimental details, gas adsorption data and X-ray powder diffraction data. See DOI: 10.1039/b000000x/

1. O. M. Yaghi, J. Kim, M. O'Keefe, R. Q. Snurr, A. O. Yazaydin, E. Choi, S. B. Choi, N. Aratani, Y. B. Go, N. Ko and H. Furukawa, *Science*, 2010, **329**, 424-428.
2. H. Deng, S. Grunder, K. E. Cordova, C. Valente, H. Furukawa, M. Hmadeh, F. Gandara, A. C. Whalley, Z. Liu, S. Asahina, H. Kazumori, M. O'Keeffe, O. Terasaki, J. F. Stoddart and O. M. Yaghi, *Science*, 2012, **336**, 1018-1023.
3. G. Ferey, D. Louer, G. Marsolier, M. Nogues, C. Thouvenot, F. Millange and C. Serre, *J. Am. Chem. Soc.*, 2002, **124**, 13519-13526.
4. O. M. Yaghi, M. O'Keefe, M. Eddaoudi and H. Li, *Nature*, 1999, **402**, 276-279.
5. M. Eddaoudi, H. Li and O. M. Yaghi, *J. Am. Chem. Soc.*, 2000, **122**, 1391-1397.
6. S. S.-Y. Chui, S. M.-F. Lo, J. P. H. Charmant, A. G. Orpen and I. D. Williams, *Science*, 1999, **283**, 1148-1150.
7. M. Kondo, T. Yoshitomi, H. Matsuzaka, S. Kitagawa and K. Seki, *Angew. Chem. Int. Ed. Engl.*, 1997, **36**, 1725-1727.
8. M. Fujita, Y. J. Kwon, S. Washizu and K. Ogura, *J. Am. Chem. Soc.*, 1994, **116**, 1151-1152.
9. M. O'Keefe, N. W. Ockwig, H. K. Chae, M. Eddaoudi, J. Kim and O. M. Yaghi, *Nature*, 2003, **423**, 705-714.
10. W. M. Bloch and C. J. Sumby, *Chem. Commun.*, 2012, **48**, 2534-2536.
11. Y. Cheng, A. Kondo, H. Noguchi, H. Kajiro, K. Urita, T. Ohba, K. Kaneko and H. Kanoh, *Langmuir*, 2009, **25**, 4510-4513.
12. R. Kotani, A. Kondo and K. Maeda, *Chem. Commun.*, 2012, **48**, 11316-11318.
13. F.-X. Coudert, C. Mellot-Draznieks, A. H. Fuchs and A. Boutin, *J. Am. Chem. Soc.*, 2009, **131**, 11329-11331.
14. Y. Liu, H. Kabbour, C. M. Brown, D. A. Neumann and C. C. Ahn, *Langmuir*, 2008, **24**, 4772-4777.
15. N. L. Rosi, J. Kim, M. Eddaoudi, B. Chen, M. O'Keefe and O. M. Yaghi, *J. Am. Chem. Soc.*, 2005, **127**, 1504-1518.
16. B. Xiao, P. S. Wheatley, X. Zhao, A. J. Fletcher, S. Fox, A. G. Rossi, I. L. Megson, S. Bordiga, L. Regli, K. M. Thomas and R. E. Morris, *J. Am. Chem. Soc.*, 2007, **129**, 1203-1209.
17. D. F. Sava, K. W. Chapman, M. A. Rodriguez, J. A. Greathouse, P. S. Crozier, H. Zhao, P. J. Chupas and T. M. Nenoff, *Chem. Mater.*, 2013, **5**, 2591–2596.
18. E. D. Bloch, W. L. Queen, R. Krishna, J. M. Zadrozny, C. M. Brown and J. R. Long, *Science*, 2012, **335**, 1606-1610.
19. W. L. Queen, E. D. Bloch, C. M. Brown, M. R. Hudson, J. A. Mason, L. J. Murray, A. J. Ramirez-Cuesta, V. K. Peterson and J. R. Long, *Dalton Trans.*, 2012, **41**, 4180-4187.
20. D. Britt, H. Furukawa, B. Wang, T. G. Glover and O. M. Yaghi, *Proc. Nat. Acad. Sci.*, 2009, **106**, 20637-20640.
21. D. Rankine, A. Avellaneda, M. R. Hill, C. J. Doonan and C. J. Sumby, *Chem. Commun.*, 2012, **48**, 10328-10330.
22. T. D. Keene, D. Rankine, J. D. Evans, P. D. Southon, C. J. Kepert, J. B. Aitken, C. J. Sumby and C. J. Doonan, *Dalton Trans.*, 2013, **42**, 7871-7879.
23. T. Kundu, S. C. Sahoo and R. Banerjee, *Chem. Commun.*, 2012, **48**, 4998-5000.
24. T. M. McDonald, W. R. Lee, J. A. Mason, B. M. Wiers, C. S. Hong and J. R. Long, *J. Am. Chem. Soc.*, 2012, **134**, 7056-7065.
25. T. R. Cook, Y.-R. Zheng and P. J. Stang, *Chem. Rev.*, 2013, **113**, 734-777.
26. N. Stock and S. Biswas, *Chem. Rev.*, 2012, **112**, 933-969.
27. L. E. Kreno, K. Leong, O. K. Farha, M. Allendorf, R. P. Van Duyne and J. T. Hupp, *Chem. Rev.*, 2012, **112**, 1105-1125.
28. G. M. Sheldrick, *SHELXL-97*, University of Gottingen, Gottingen, Germany, 1997.
29. G. M. Sheldrick, *Acta. Cryst.*, 1990, **A46**, 467-473.

View Article Online
DOI: 10.1039/C3CE41253A

30. L. J. Barbour, *J. Supramol. Chem.*, 2001, **1**, 189-191.
31. Q. Zhang, H. Hao, H. Zhang, S. Wang, J. Jin and D. Sun, *Eur. J. Inorg. Chem.*, 2013, **2013**, 1123-1126.
32. B. Liu, R. Shang, K.-L. Hu, Z.-M. Wang and S. Gao, *Inorg. Chem.*, 2012, **51**, 13363-13372.
33. S. Yu and L. Pu, *J. Am. Chem. Soc.*, 2010, **132**, 17698-17700.
34. L. Pu, *Acc. Chem. Res.*, 2011, **45**, 150-163.

View Article Online
DOI: 10.1039/C3CE41253A

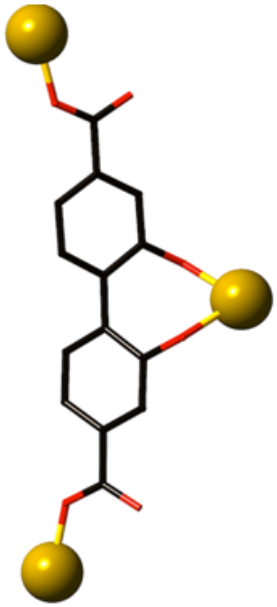

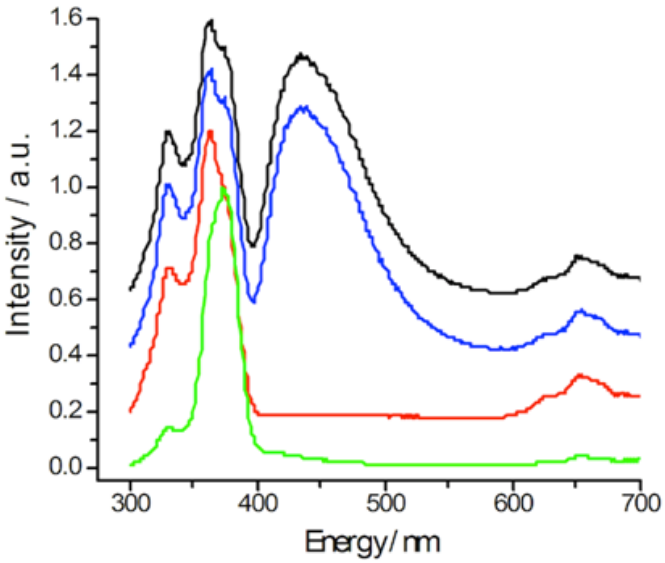

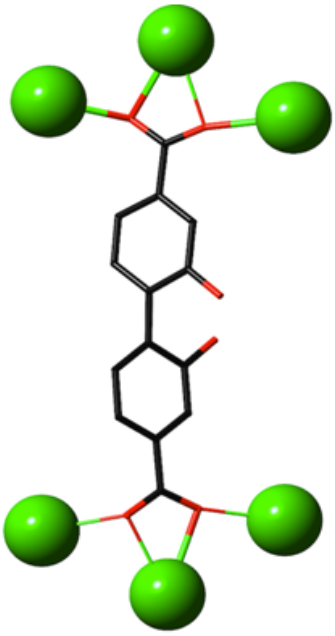

OFF

ON